


Search for a strangeonium-like structure Z_s decaying into $\phi\pi$ and a measurement of the cross section $e^+e^- \rightarrow \phi\pi\pi$

M. Ablikim,¹ M. N. Achasov,^{9,d} S. Ahmed,¹⁴ M. Albrecht,⁴ A. Amoroso,^{53a,53c} F. F. An,¹ Q. An,^{50,40} J. Z. Bai,¹ Y. Bai,³⁹ O. Bakina,²⁴ R. Baldini Ferroli,^{20a} Y. Ban,³² D. W. Bennett,¹⁹ J. V. Bennett,⁵ N. Berger,²³ M. Bertani,^{20a} D. Bettoni,^{21a} J. M. Bian,⁴⁷ F. Bianchi,^{53a,53c} E. Boger,^{24,b} I. Boyko,²⁴ R. A. Briere,⁵ H. Cai,⁵⁵ X. Cai,^{1,40} O. Cakir,^{43a} A. Calcaterra,^{20a} G. F. Cao,^{1,44} S. A. Cetin,^{43b} J. Chai,^{53c} J. F. Chang,^{1,40} G. Chelkov,^{24,b,c} G. Chen,¹ H. S. Chen,^{1,44} J. C. Chen,¹ M. L. Chen,^{1,40} P. L. Chen,⁵¹ S. J. Chen,³⁰ X. R. Chen,²⁷ Y. B. Chen,^{1,40} X. K. Chu,³² G. Cibinetto,^{21a} H. L. Dai,^{1,40} J. P. Dai,^{35,h} A. Dbeyssi,¹⁴ D. Dedovich,²⁴ Z. Y. Deng,¹ A. Denig,²³ I. Denysenko,²⁴ M. Destefanis,^{53a,53c} F. De Mori,^{53a,53c} Y. Ding,²⁸ C. Dong,³¹ J. Dong,^{1,40} L. Y. Dong,^{1,44} M. Y. Dong,^{1,40,44} Z. L. Dou,³⁰ S. X. Du,⁵⁷ P. F. Duan,¹ J. Fang,^{1,40} S. S. Fang,^{1,44} Y. Fang,¹ R. Farinelli,^{21a,21b} L. Fava,^{53b,53c} S. Fegan,²³ F. Feldbauer,²³ G. Felici,^{20a} C. Q. Feng,^{50,40} E. Fioravanti,^{21a} M. Fritsch,^{23,14} C. D. Fu,¹ Q. Gao,¹ X. L. Gao,^{50,40} Y. Gao,⁴² Y. G. Gao,⁶ Z. Gao,^{50,40} I. Garzia,^{21a} K. Goetzen,¹⁰ L. Gong,³¹ W. X. Gong,^{1,40} W. Gradl,²³ M. Greco,^{53a,53c} M. H. Gu,^{1,40} Y. T. Gu,¹² A. Q. Guo,¹ R. P. Guo,^{1,44} Y. P. Guo,²³ Z. Haddadi,²⁶ S. Han,⁵⁵ X. Q. Hao,¹⁵ F. A. Harris,⁴⁵ K. L. He,^{1,44} X. Q. He,⁴⁹ F. H. Heinsius,⁴ T. Held,⁴ Y. K. Heng,^{1,40,44} T. Holtmann,⁴ Z. L. Hou,¹ H. M. Hu,^{1,44} T. Hu,^{1,40,44} Y. Hu,¹ G. S. Huang,^{50,40} J. S. Huang,¹⁵ X. T. Huang,³⁴ X. Z. Huang,³⁰ Z. L. Huang,²⁸ T. Hussain,⁵² W. Ikegami Andersson,⁵⁴ Q. Ji,¹ Q. P. Ji,¹⁵ X. B. Ji,^{1,44} X. L. Ji,^{1,40} X. S. Jiang,^{1,40,44} X. Y. Jiang,³¹ J. B. Jiao,³⁴ Z. Jiao,¹⁷ D. P. Jin,^{1,40,44} S. Jin,^{1,44} Y. Jin,⁴⁶ T. Johansson,⁵⁴ A. Julin,⁴⁷ N. Kalantar-Nayestanaki,²⁶ X. L. Kang,^{1,*} X. S. Kang,³¹ M. Kavatsyuk,²⁶ B. C. Ke,⁵ T. Khan,^{50,40} A. Khoukaz,⁴⁸ P. Kiese,²³ R. Kliemt,¹⁰ L. Koch,²⁵ O. B. Kolcu,^{43b,f} B. Kopf,⁴ M. Kornicer,⁴⁵ M. Kuemmel,⁴ M. Kuessner,⁴ M. Kuhlmann,⁴ A. Kupsc,⁵⁴ W. Kühn,²⁵ J. S. Lange,²⁵ M. Lara,¹⁹ P. Larin,¹⁴ L. Lavezzi,^{53c} H. Leithoff,²³ C. Leng,^{53c} C. Li,⁵⁴ Cheng Li,^{50,40} D. M. Li,⁵⁷ F. Li,^{1,40} F. Y. Li,³² G. Li,¹ H. B. Li,^{1,44} H. J. Li,^{1,44} J. C. Li,¹ Jin Li,³³ K. J. Li,⁴¹ Kang Li,¹³ Ke Li,³⁴ Lei Li,³ P. L. Li,^{50,40} P. R. Li,^{44,7} Q. Y. Li,³⁴ W. D. Li,^{1,44} W. G. Li,¹ X. L. Li,³⁴ X. N. Li,^{1,40} X. Q. Li,³¹ Z. B. Li,⁴¹ H. Liang,^{50,40} Y. F. Liang,³⁷ Y. T. Liang,²⁵ G. R. Liao,¹¹ D. X. Lin,¹⁴ B. Liu,^{35,h} B. J. Liu,¹ C. X. Liu,¹ D. Liu,^{50,40} F. H. Liu,³⁶ Fang Liu,^{1,†} Feng Liu,⁶ H. B. Liu,¹² H. M. Liu,^{1,44} Huanhuan Liu,¹ Huihui Liu,¹⁶ J. B. Liu,^{50,40} J. P. Liu,⁵⁵ J. Y. Liu,^{1,44} K. Liu,⁴² K. Y. Liu,²⁸ Ke Liu,⁶ L. D. Liu,³² P. L. Liu,^{1,40} Q. Liu,⁴⁴ S. B. Liu,^{50,40} X. Liu,²⁷ Y. B. Liu,³¹ Z. A. Liu,^{1,40,44} Zhiqing Liu,²³ Y. F. Long,³² X. C. Lou,^{1,40,44} H. J. Lu,¹⁷ J. G. Lu,^{1,40} Y. Lu,¹ Y. P. Lu,^{1,40} C. L. Luo,²⁹ M. X. Luo,⁵⁶ X. L. Luo,^{1,40} X. R. Lyu,⁴⁴ F. C. Ma,²⁸ H. L. Ma,¹ L. L. Ma,³⁴ M. M. Ma,^{1,44} Q. M. Ma,¹ T. Ma,¹ X. N. Ma,³¹ X. Y. Ma,^{1,40} Y. M. Ma,³⁴ F. E. Maas,¹⁴ M. Maggiora,^{53a,53c} Q. A. Malik,⁵² Y. J. Mao,³² Z. P. Mao,¹ S. Marcello,^{53a,53c} Z. X. Meng,⁴⁶ J. G. Messchendorp,²⁶ G. Mezzadri,^{21b} J. Min,^{1,40} T. J. Min,¹ R. E. Mitchell,¹⁹ X. H. Mo,^{1,40,44} Y. J. Mo,⁶ C. Morales Morales,¹⁴ N. Yu. Muchnoi,^{9,d} H. Muramatsu,⁴⁷ A. Mustafa,⁴ Y. Nefedov,²⁴ F. Nerling,¹⁰ I. B. Nikolaev,^{9,d} Z. Ning,^{1,40} S. Nisar,⁸ S. L. Niu,^{1,40} X. Y. Niu,^{1,44} S. L. Olsen,^{33,j} Q. Ouyang,^{1,40,44} S. Pacetti,^{20b} Y. Pan,^{50,40} M. Papenbrock,⁵⁴ P. Patteri,^{20a} M. Pelizaeus,⁴ J. Pellegrino,^{53a,53c} H. P. Peng,^{50,40} K. Peters,^{10,g} J. Pettersson,⁵⁴ J. L. Ping,²⁹ R. G. Ping,^{1,44} A. Pitka,²³ R. Poling,⁴⁷ V. Prasad,^{50,40} H. R. Qi,² M. Qi,³⁰ S. Qian,^{1,40} C. F. Qiao,⁴⁴ N. Qin,⁵⁵ X. S. Qin,⁴ Z. H. Qin,^{1,40} J. F. Qiu,¹ K. H. Rashid,^{52,i} C. F. Redmer,²³ M. Richter,⁴ M. Ripka,²³ M. Rolo,^{53c} G. Rong,^{1,44} Ch. Rosner,¹⁴ A. Sarantsev,^{24,e} M. Savrić,^{21b} C. Schnier,⁴ K. Schoenning,⁵⁴ W. Shan,³² M. Shao,^{50,40} C. P. Shen,² P. X. Shen,³¹ X. Y. Shen,^{1,44} H. Y. Sheng,¹ J. J. Song,³⁴ W. M. Song,³⁴ X. Y. Song,¹ S. Sosio,^{53a,53c} C. Sowa,⁴ S. Spataro,^{53a,53c} G. X. Sun,¹ J. F. Sun,¹⁵ L. Sun,⁵⁵ S. S. Sun,^{1,44} X. H. Sun,¹ Y. J. Sun,^{50,40} Y. K. Sun,^{50,40} Y. Z. Sun,¹ Z. J. Sun,^{1,40} Z. T. Sun,¹⁹ C. J. Tang,³⁷ G. Y. Tang,¹ X. Tang,¹ I. Tapan,^{43c} M. Tiemens,²⁶ B. Tsednee,²² I. Uman,^{43d} G. S. Varner,⁴⁵ B. Wang,¹ B. L. Wang,⁴⁴ D. Wang,³² D. Y. Wang,³² Dan Wang,⁴⁴ K. Wang,^{1,40} L. L. Wang,¹ L. S. Wang,¹ M. Wang,³⁴ Meng Wang,^{1,44} P. Wang,¹ P. L. Wang,¹ W. P. Wang,^{50,40} X. F. Wang,⁴² Y. Wang,³⁸ Y. D. Wang,¹⁴ Y. F. Wang,^{1,40,44} Y. Q. Wang,²³ Z. Wang,^{1,40} Z. G. Wang,^{1,40} Z. Y. Wang,¹ Zongyuan Wang,^{1,44} T. Weber,²³ D. H. Wei,¹¹ P. Weidenkaff,²³ S. P. Wen,¹ U. Wiedner,⁴ M. Wolke,⁵⁴ L. H. Wu,¹ L. J. Wu,^{1,44} Z. Wu,^{1,40} L. Xia,^{50,40} Y. Xia,¹⁸ D. Xiao,¹ H. Xiao,⁵¹ Y. J. Xiao,^{1,44} Z. J. Xiao,²⁹ Y. G. Xie,^{1,40} Y. H. Xie,⁶ X. A. Xiong,^{1,44} Q. L. Xiu,^{1,40} G. F. Xu,¹ J. J. Xu,^{1,44} L. Xu,¹ Q. J. Xu,¹³ Q. N. Xu,⁴⁴ X. P. Xu,³⁸ L. Yan,^{53a,53c} W. B. Yan,^{50,40} W. C. Yan,² Y. H. Yan,¹⁸ H. J. Yang,^{35,h} H. X. Yang,¹ L. Yang,⁵⁵ Y. H. Yang,³⁰ Y. X. Yang,¹¹ M. Ye,^{1,40} M. H. Ye,⁷ J. H. Yin,¹ Z. Y. You,⁴¹ B. X. Yu,^{1,40,44} C. X. Yu,³¹ J. S. Yu,²⁷ C. Z. Yuan,^{1,44} Y. Yuan,¹ A. Yuncu,^{43b,a} A. A. Zafar,⁵² Y. Zeng,¹⁸ Z. Zeng,^{50,40} B. X. Zhang,¹ B. Y. Zhang,^{1,40} C. C. Zhang,¹ D. H. Zhang,¹ H. H. Zhang,⁴¹ H. Y. Zhang,^{1,40} J. Zhang,^{1,44} J. L. Zhang,¹ J. Q. Zhang,¹ J. W. Zhang,^{1,40,44} J. Y. Zhang,¹ J. Z. Zhang,^{1,44} K. Zhang,^{1,44} L. Zhang,⁴² S. Q. Zhang,³¹ X. Y. Zhang,³⁴ Y. H. Zhang,^{1,40} Y. T. Zhang,^{50,40} Yang Zhang,¹ Yao Zhang,¹ Yu Zhang,⁴⁴ Z. H. Zhang,⁶ Z. P. Zhang,⁵⁰ Z. Y. Zhang,⁵⁵ G. Zhao,¹ J. W. Zhao,^{1,40} J. Y. Zhao,^{1,44} J. Z. Zhao,^{1,40} Lei Zhao,^{50,40} Ling Zhao,¹ M. G. Zhao,³¹ Q. Zhao,¹ S. J. Zhao,⁵⁷ T. C. Zhao,¹ Y. B. Zhao,^{1,40} Z. G. Zhao,^{50,40} A. Zhemchugov,^{24,b} B. Zheng,⁵¹ J. P. Zheng,^{1,40} W. J. Zheng,³⁴ Y. H. Zheng,⁴⁴ B. Zhong,²⁹ L. Zhou,^{1,40} X. Zhou,⁵⁵ X. K. Zhou,^{50,40} X. R. Zhou,^{50,40} X. Y. Zhou,¹ Y. X. Zhou,¹² J. Zhu,³¹ J. Zhu,⁴¹ K. Zhu,¹ K. J. Zhu,^{1,40,44} S. Zhu,¹ S. H. Zhu,⁴⁹ X. L. Zhu,⁴² Y. C. Zhu,^{50,40} Y. S. Zhu,^{1,44} Z. A. Zhu,^{1,44} J. Zhuang,^{1,40} B. S. Zou,¹ and J. H. Zou¹

(BESIII Collaboration)

- ¹*Institute of High Energy Physics, Beijing 100049, People's Republic of China*
²*Beihang University, Beijing 100191, People's Republic of China*
³*Beijing Institute of Petrochemical Technology, Beijing 102617, People's Republic of China*
⁴*Bochum Ruhr-University, D-44780 Bochum, Germany*
⁵*Carnegie Mellon University, Pittsburgh, Pennsylvania 15213, USA*
⁶*Central China Normal University, Wuhan 430079, People's Republic of China*
⁷*China Center of Advanced Science and Technology, Beijing 100190, People's Republic of China*
⁸*COMSATS Institute of Information Technology, Lahore, Defence Road, Off Raiwind Road, 54000 Lahore, Pakistan*
⁹*G.I. Budker Institute of Nuclear Physics SB RAS (BINP), Novosibirsk 630090, Russia*
¹⁰*GSI Helmholtzcentre for Heavy Ion Research GmbH, D-64291 Darmstadt, Germany*
¹¹*Guangxi Normal University, Guilin 541004, People's Republic of China*
¹²*Guangxi University, Nanning 530004, People's Republic of China*
¹³*Hangzhou Normal University, Hangzhou 310036, People's Republic of China*
¹⁴*Helmholtz Institute Mainz, Johann-Joachim-Becher-Weg 45, D-55099 Mainz, Germany*
¹⁵*Henan Normal University, Xinxiang 453007, People's Republic of China*
¹⁶*Henan University of Science and Technology, Luoyang 471003, People's Republic of China*
¹⁷*Huangshan College, Huangshan 245000, People's Republic of China*
¹⁸*Human University, Changsha 410082, People's Republic of China*
¹⁹*Indiana University, Bloomington, Indiana 47405, USA*
^{20a}*INFN Laboratori Nazionali di Frascati, I-00044 Frascati, Italy*
^{20b}*INFN and University of Perugia, I-06100 Perugia, Italy*
^{21a}*INFN Sezione di Ferrara, I-44122 Ferrara, Italy*
^{21b}*University of Ferrara, I-44122 Ferrara, Italy*
²²*Institute of Physics and Technology, Peace Ave. 54B, Ulaanbaatar 13330, Mongolia*
²³*Johannes Gutenberg University of Mainz, Johann-Joachim-Becher-Weg 45, D-55099 Mainz, Germany*
²⁴*Joint Institute for Nuclear Research, 141980 Dubna, Moscow region, Russia*
²⁵*Justus-Liebig-Universitaet Giessen, II. Physikalisches Institut, Heinrich-Buff-Ring 16, D-35392 Giessen, Germany*
²⁶*KVI-CART, University of Groningen, NL-9747 AA Groningen, The Netherlands*
²⁷*Lanzhou University, Lanzhou 730000, People's Republic of China*
²⁸*Liaoning University, Shenyang 110036, People's Republic of China*
²⁹*Nanjing Normal University, Nanjing 210023, People's Republic of China*
³⁰*Nanjing University, Nanjing 210093, People's Republic of China*
³¹*Nankai University, Tianjin 300071, People's Republic of China*
³²*Peking University, Beijing 100871, People's Republic of China*
³³*Seoul National University, Seoul 151-747, Korea*
³⁴*Shandong University, Jinan 250100, People's Republic of China*
³⁵*Shanghai Jiao Tong University, Shanghai 200240, People's Republic of China*
³⁶*Shanxi University, Taiyuan 030006, People's Republic of China*
³⁷*Sichuan University, Chengdu 610064, People's Republic of China*
³⁸*Soochow University, Suzhou 215006, People's Republic of China*
³⁹*Southeast University, Nanjing 211100, People's Republic of China*
⁴⁰*State Key Laboratory of Particle Detection and Electronics, Beijing 100049, Hefei 230026, People's Republic of China*
⁴¹*Sun Yat-Sen University, Guangzhou 510275, People's Republic of China*
⁴²*Tsinghua University, Beijing 100084, People's Republic of China*
^{43a}*Ankara University, 06100 Tandogan, Ankara, Turkey*
^{43b}*Istanbul Bilgi University, 34060 Eyup, Istanbul, Turkey*
^{43c}*Uludag University, 16059 Bursa, Turkey*
^{43d}*Near East University, Nicosia, North Cyprus, Mersin 10, Turkey*
⁴⁴*University of Chinese Academy of Sciences, Beijing 100049, People's Republic of China*
⁴⁵*University of Hawaii, Honolulu, Hawaii 96822, USA*
⁴⁶*University of Jinan, Jinan 250022, People's Republic of China*
⁴⁷*University of Minnesota, Minneapolis, Minnesota 55455, USA*
⁴⁸*University of Muenster, Wilhelm-Klemm-Str. 9, 48149 Muenster, Germany*
⁴⁹*University of Science and Technology Liaoning, Anshan 114051, People's Republic of China*

⁵⁰University of Science and Technology of China, Hefei 230026, People's Republic of China⁵¹University of South China, Hengyang 421001, People's Republic of China⁵²University of the Punjab, Lahore-54590, Pakistan^{53a}University of Turin, I-10125, Turin, Italy^{53b}University of Eastern Piedmont, I-15121, Alessandria, Italy^{53c}INFN, I-10125, Turin, Italy⁵⁴Uppsala University, Box 516, SE-75120 Uppsala, Sweden⁵⁵Wuhan University, Wuhan 430072, People's Republic of China⁵⁶Zhejiang University, Hangzhou 310027, People's Republic of China⁵⁷Zhengzhou University, Zhengzhou 450001, People's Republic of China (Received 1 February 2018; revised manuscript received 17 October 2018; published 18 January 2019)

Using a data sample of e^+e^- collision data corresponding to an integrated luminosity of 108 pb^{-1} collected with the BESIII detector at a center-of-mass energy of 2.125 GeV, we study the process $e^+e^- \rightarrow \phi\pi\pi$ and search for a strangeoniumlike structure Z_s decaying into $\phi\pi$. No signal is observed in the $\phi\pi$ mass spectrum. Upper limits on the cross sections for Z_s production at the 90% confidence level are determined. In addition, the cross sections of $e^+e^- \rightarrow \phi\pi^+\pi^-$ and $e^+e^- \rightarrow \phi\pi^0\pi^0$ at 2.125 GeV are measured to be $(436.2 \pm 6.4 \pm 30.1) \text{ pb}$ and $(237.0 \pm 8.6 \pm 15.4) \text{ pb}$, respectively, where the first uncertainties are statistical and the second systematic.

DOI: [10.1103/PhysRevD.99.011101](https://doi.org/10.1103/PhysRevD.99.011101)

A charged charmoniumlike structure, $Z_c(3900)$, was observed in the $\pi^\pm J/\psi$ final states by the BESIII and Belle experiments [1,2]. Subsequently, several analogous structures were reported and confirmed by different experiments [3–7]. These observations inspired extensive discussions of their nature, and the reasonable interpretations are tetraquark states, molecular or hadroquarkonium

states [8–14], due to these structures carrying charge and prominently decaying into a pion and a conventional charmonium state. More recently, the neutral partners of these charmoniumlike structures were observed [15–18], which indicate the isotriplet property of these structures and hint of a new hadron spectroscopy.

By replacing the $c\bar{c}$ pair in the Z_c structure with an $s\bar{s}$, it is possible to consider an analogous Z_s structure. Similar to $Y(4260) \rightarrow J/\psi\pi^+\pi^-$ in which the $Z_c(3900)$ was observed [1,2], the process $\phi(2170) \rightarrow \phi\pi^+\pi^-$ is considered as a unique place to search for the Z_s structure, as the $\phi(2170)$ is regarded as the strangeoniumlike states analogy to $Y(4260)$ in charmonium sector [19]. Furthermore, the conventional isosinglet $s\bar{s}$ state decaying into $\phi\pi$ is suppressed by the conservation of isospin symmetry, while for a conventional meson composed of u, d quarks, the $\phi\pi$ decay mode is strongly suppressed by the Okubo-Zweig-Iizuka (OZI) rule [20]. Therefore, it is of interest to perform an experimental search for the strangeoniumlike structure Z_s since its observation may imply the existence of an exotic state.

In this article, we present a search for the Z_s structure in the process $e^+e^- \rightarrow \phi\pi\pi$ using a data sample corresponding to an integrated luminosity of $(108.49 \pm 0.75) \text{ pb}^{-1}$ [21], taken at a center-of-mass energy of 2.125 GeV with the BESIII detector. Since the observed $Z_c(3900)$ [1,2] and $Z_c(3885)$ [5] are close to the $D^*\bar{D}$ mass threshold and have a narrow width, the search for a narrow width Z_s structure around the $K^*\bar{K}$ mass threshold ($1.4 \text{ GeV}/c^2$) in the $\phi\pi$ mass spectrum allows us to test the novel scenario of the initial single pion emission mechanism (ISPE) [22].

The BESIII detector [23] is a magnetic spectrometer located at the Beijing Electron Position Collider (BEPCII), which is a double-ring e^+e^- collider with a peak luminosity

*Corresponding author.

kangxl@ihep.ac.cn

†Corresponding author.

liufang@ihep.ac.cn

^aAlso at Bogazici University, 34342 Istanbul, Turkey.^bAlso at the Moscow Institute of Physics and Technology, Moscow 141700, Russia.^cAlso at the Functional Electronics Laboratory, Tomsk State University, Tomsk 634050, Russia.^dAlso at the Novosibirsk State University, Novosibirsk 630090, Russia.^eAlso at the NRC “Kurchatov Institute”, PNPI, Gatchina 188300, Russia.^fAlso at Istanbul Arel University, 34295 Istanbul, Turkey.^gAlso at Goethe University Frankfurt, 60323 Frankfurt am Main, Germany.^hAlso at Key Laboratory for Particle Physics, Astrophysics and Cosmology, Ministry of Education; Shanghai Key Laboratory for Particle Physics and Cosmology; Institute of Nuclear and Particle Physics, Shanghai 200240, People's Republic of China.ⁱGovernment College Women University, Sialkot—51310, Punjab, Pakistan.^jCurrently at: Center for Underground Physics, Institute for Basic Science, Daejeon 34126, Korea.

Published by the American Physical Society under the terms of the [Creative Commons Attribution 4.0 International license](https://creativecommons.org/licenses/by/4.0/). Further distribution of this work must maintain attribution to the author(s) and the published article's title, journal citation, and DOI. Funded by SCOAP³.

of $10^{33} \text{ cm}^{-2} \text{ s}^{-1}$ at a center-of-mass energy of 3.773 GeV. The cylindrical core of the BESIII detector consists of a helium-based multilayer drift chamber (MDC), a plastic scintillator time-of-flight system (TOF), and a CsI (TI) electromagnetic calorimeter (EMC), which are all immersed in a superconducting solenoidal magnet providing a 1.0 T magnetic field. The solenoid is supported by an octagonal flux-return yoke with resistive plate counter muon identifier (MUC) modules interleaved with steel. The acceptance of charged particles is 93% over 4π solid angle. The charged-particle momentum resolution at 1 GeV/c is 0.5%, and the specific energy loss (dE/dx) resolution is 6%. The EMC measures photon energies with a resolution of 2.5% (5%) at 1 GeV in the barrel (end caps) region. The time resolution of TOF is 80 ps in the barrel and 110 ps in the end caps. The position resolution in the MUC is better than 2 cm.

The GEANT4-based [24] Monte Carlo (MC) simulation software, which includes the geometric description of the BESIII detector and the detector response, is used to determine the detection efficiencies and estimate backgrounds. To simulate the $e^+e^- \rightarrow \phi\pi\pi$ process, the line-shape reported by *BABAR* [25] is adopted. Intermediate states in the simulation of $e^+e^- \rightarrow \phi\pi\pi$ process are modeled according to the BESIII data as described later.

Candidate events of $e^+e^- \rightarrow \phi\pi^+\pi^-$ ($\phi \rightarrow K^+K^-$) are required to have three or four charged tracks. Charged tracks are reconstructed from hits in the MDC within the polar angle range $|\cos\theta| < 0.93$. The tracks are required to pass the interaction point within 10 cm along the beam direction and within 1 cm in the plane perpendicular to the beam. For each charged track, the TOF and the dE/dx information are combined to form particle identification (PID) confidence levels (C.L.) for the π , K , and p hypotheses, and the particle type with the highest C.L. is assigned to each track. Two pions with opposite charges and at least one kaon are required to be identified. A one-constraint (1C) kinematic fit is performed under the hypothesis that the $K\pi^+\pi^-$ missing mass corresponds to the kaon mass, and the corresponding χ^2 , denoted as $\chi^2_{1C}(\pi^+\pi^-KK_{\text{miss}})$, is required to be less than 10. For events with two reconstructed and identified kaons, the combination with the smaller $\chi^2_{1C}(\pi^+\pi^-KK_{\text{miss}})$ is retained.

Candidate events of $e^+e^- \rightarrow \phi\pi^0\pi^0$ ($\phi \rightarrow K^+K^-$, $\pi^0 \rightarrow \gamma\gamma$) are required to have one or two charged tracks and at least four photon candidates. Photon candidates are reconstructed from isolated showers in the EMC, and the corresponding energies are required to be at least 25 MeV in the barrel ($|\cos\theta| < 0.80$) or 50 MeV in the end caps ($0.86 < |\cos\theta| < 0.92$). To eliminate showers associated with charged particles, the angle between the cluster and the nearest charged track must be larger than 10 degrees. An EMC cluster timing requirement of $0 \leq t \leq 700$ ns is also applied to suppress electronic noise and energy deposits unrelated to the event. At least one kaon is

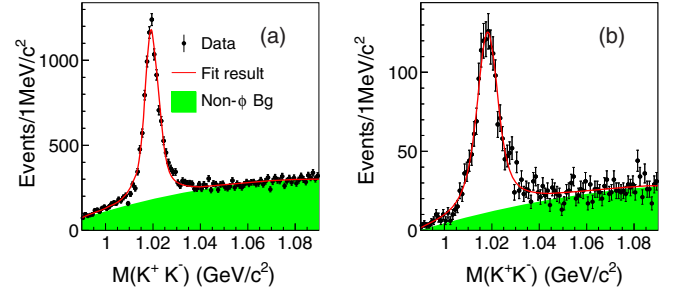


FIG. 1. Invariant mass distributions of K^+K^- for (a) $e^+e^- \rightarrow K^+K^-\pi^+\pi^-$ and (b) $e^+e^- \rightarrow K^+K^-\pi^0\pi^0$ events. The dots with error bars are data, the solid lines are the fit results and the shaded parts are the combinatorial backgrounds obtained from fits.

required to be identified. A 1C kinematic fit is then performed under the hypothesis that the $K4\gamma$ missing mass is the kaon mass. For events with two identified kaons or more than four photons, the combination with the smallest $\chi^2_{1C}(4\gamma KK_{\text{miss}})$ is retained and required to be less than 20. The four selected photons are grouped into pairs to form π^0 mesons. Two π^0 candidates are then selected by minimizing the quantity $(M(\gamma\gamma)_1 - m_{\pi^0})^2 + (M(\gamma\gamma)_2 - m_{\pi^0})^2$, where m_{π^0} is the nominal π^0 mass from Particle Data Group (PDG) [26]. In order to select a clean sample, both $M(\gamma\gamma)_1$ and $M(\gamma\gamma)_2$ are required to be within ± 20 MeV/c² of m_{π^0} .

After applying the above selection criteria, the K^+K^- invariant mass, $M(K^+K^-)$, is computed using the four-momenta of the reconstructed K and K_{miss} from the kinematic fit. The $M(K^+K^-)$ spectra for the selected candidate events are shown in Figs. 1(a) and 1(b), where ϕ signals are clearly seen. The Dalitz plots of the $\phi\pi^+\pi^-$ and $\phi\pi^0\pi^0$ events are shown in Figs. 2(a) and 2(b), respectively, where the $M(K^+K^-)$ is required to be in the ϕ mass range, $|M(K^+K^-) - m_\phi| < 0.01$ GeV/c², and m_ϕ is the nominal ϕ mass from PDG [26]. The apparent structures are from the decay processes $e^+e^- \rightarrow \phi f_0(980)$ with $f_0(980)$ decaying to $\pi^+\pi^-$ or $\pi^0\pi^0$ final states, which are also clearly indicated in the $\pi\pi$ invariant mass spectra, $M(\pi\pi)$, displayed in Figs. 2(c) and 2(d). There is a clear structure around ρ mass region in the $\pi\pi$ mass spectrum in the $K^+K^-\pi^+\pi^-$ channel. In addition, $K^*(892)K^\mp\pi^\pm$ events also contaminate the charged process. The contributions from those non- ϕ backgrounds are described by the events in the ϕ sideband regions, $0.995 < M(K^+K^-) < 1.005$ and $1.035 < M(K^+K^-) < 1.045$ GeV/c², and are normalized according to the fitted intensities in Fig. 1. The $M(\pi\pi)$ distributions of ϕ sideband events are represented by the dotted lines in Figs. 2(c) and 2(d).

The mass spectra of the ϕ candidate paired with π are shown in Fig. 3. There is no evidence of structures in the entire $\phi\pi$ region. To describe the $M(\pi\pi)$ spectrum, an amplitude analysis on $e^+e^- \rightarrow \phi\pi\pi$ is performed using the relativistic covariant tensor amplitude method [27].

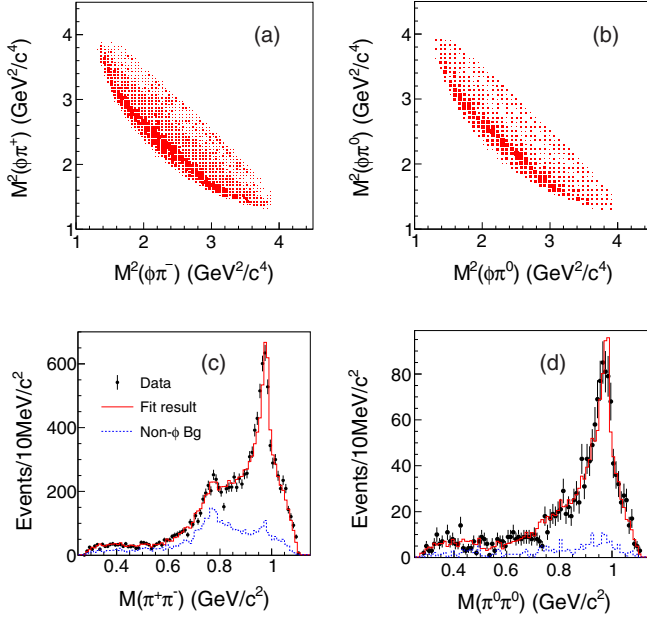


FIG. 2. Dalitz plots for (a) $e^+e^- \rightarrow \phi\pi^+\pi^-$ and (b) $e^+e^- \rightarrow \phi\pi^0\pi^0$ candidate events and invariant mass distributions of (c) $\pi^+\pi^-$ and (d) $\pi^0\pi^0$. The dots with error bars are data, the dotted histograms are non- ϕ backgrounds estimated from ϕ sidebands, and the solid histograms are the sum of the projections of the amplitude analysis results and non- ϕ backgrounds. Each $e^+e^- \rightarrow \phi\pi^0\pi^0$ event contributes two entries for (b).

The $e^+e^- \rightarrow \phi\pi\pi$ process can be described by four subprocesses: $e^+e^- \rightarrow \phi\sigma$, $\phi f_0(980)$, $\phi f_0(1370)$, and $\phi f_2(1270)$. σ is described with the form used fitting $\pi\pi$ elastic scattering data [28], $f_0(980)$ is described with a Flatté formula [29], and others are described with relativistic Breit-Winger (BW) function. The resonance parameters are fixed on the values determined in previous BES results [30,31]. Non- ϕ backgrounds estimated from the ϕ

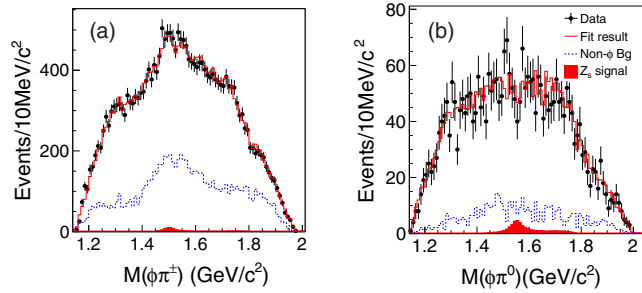


FIG. 3. Invariant mass distributions of (a) $M(\phi\pi^\pm)$ and (b) $M(\phi\pi^0)$ for $\phi\pi\pi$ candidate events. The dots with error bars are data, the solid histograms are the projections of the amplitude analysis results including the contributions from $Z_s \rightarrow \phi\pi$ process with the mass and width of Z_s^\pm (Z_s^0) assumed to be 1.5 (1.55) GeV/c^2 and 50 MeV for the case of $J^P = 1^+$, the dashed histograms are non- ϕ backgrounds, and the shaded histograms are the Z_s signal.

sidebands are represented by a non-interfering term. The projections of nominal amplitude analysis results on the $M(\pi\pi)$ distributions are shown as the solid lines in Figs. 2(c) and 2(d). The comparisons of angular distributions between data and the amplitude analysis projections for these two interested processes are also displayed in Fig. 4. To illustrate the fit quality, we present a χ^2 test for each distribution (χ^2/nbin), where nbin is the number of bins. In general the values of χ^2/nbin are around 1, which indicates that the amplitude analysis results provide a reasonable description of data.

To estimate the statistical significance for each component, alternative fits by excluding the corresponding amplitude are performed. The statistical significance is then determined by the changes of the log likelihood values and the number of degrees of freedom. The statistical significances of all these states are found to be larger than 5σ . A full partial wave analysis of $e^+e^- \rightarrow K^+K^-\pi^+\pi^-$ is in progress with more statistics taken at different energy points around $Y(2175)$ at BESIII, in which detailed results will be presented.

With a hypothesis of $J^P = 1^+$, the contribution of Z_s is examined by introducing an additional component in the amplitude analysis. To simplify the analysis, we neglect the D-wave and assume that the contribution is only from the S-wave amplitude. The Z_s is parameterized as a relativistic BW function in the $\phi\pi$ system. As the mass and width of the state are unknown, we have tested signals with masses of 1.2–1.95 GeV/c^2 in steps of 0.05 GeV/c^2 . For the width, values of 10, 20, and 50 MeV are combined with each mass. With these different signal hypotheses, we performed the fit to data and found, in general, that the observed statistical significances are less than 3σ in the explored region. For $e^+e^- \rightarrow \phi\pi^+\pi^-$, the maximum local significance is 2.7σ in the case of $M(Z_s^\pm) = 1.5 \text{ GeV}/c^2$ and $\Gamma(Z_s^\pm) = 50 \text{ MeV}$, which becomes to be 2.1σ after taking the systematic uncertainty into account, and the signal yields are determined to be 46.9 ± 21.6 . While for $e^+e^- \rightarrow \phi\pi^0\pi^0$, the maximum local significance is 3.3σ in the case of $M(Z_s^0) = 1.55 \text{ GeV}/c^2$ and $\Gamma(Z_s^0) = 50 \text{ MeV}$, which becomes to be 2.8σ after taking the systematic uncertainty into account, and the signal yields are determined to be 25.2 ± 8.9 . The corresponding projections of the amplitude analysis results on $M(\phi\pi^\pm)$ and $M(\phi\pi^0)$ are shown in Figs. 3(a) and 3(b), respectively.

In the determination of the upper limits on the number of Z_s (N_s^{UL}) for different scenarios, the same approach as that in Ref. [32] is used. For each case, the statistical uncertainty is used to determine the 90% C.L. deviation, and added to the nominal yields to obtain the corresponding upper limit on the number of Z_s signals.

The systematic uncertainties on the upper limit of Z_s signal yields associated with ϕ sideband range and the nominal $\phi\pi\pi$ model, estimated by varying the resonance parameters or replacing the $f_0(1370)$ component with a

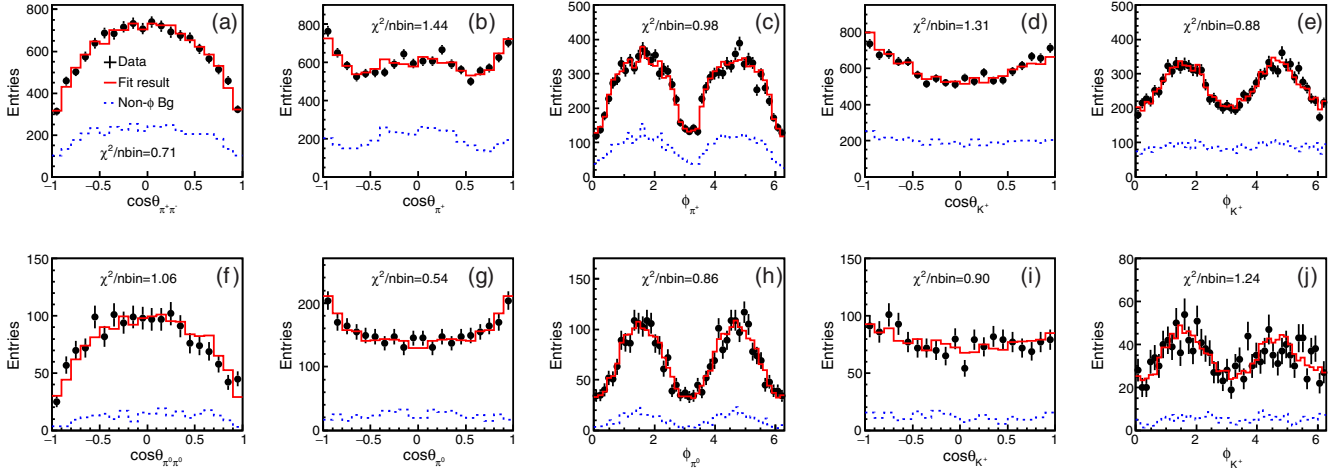


FIG. 4. Angular distributions for $e^+e^- \rightarrow \phi\pi^+\pi^-$ (a–e) and $e^+e^- \rightarrow \phi\pi^0\pi^0$ (f–j). For (g) and (h), there are two entries for each event due to the two identical π^0 s in $e^+e^- \rightarrow \phi\pi^0\pi^0$ process. The dots with error bars are data, the dotted histograms are non- ϕ backgrounds estimated from ϕ sidebands, and the solid histograms are the sum of the backgrounds and the fit projections. $\cos\theta_{\pi\pi}$ is the polar angle of $\pi\pi$ in the rest frame of e^+e^- annihilation, $\cos\theta_{\pi}$ ($\cos\theta_{K^-}$) and ϕ_{π} (ϕ_{K^-}) are the polar angle and azimuthal angle of π (K^-) in the $\pi\pi$ (K^+K^-) system.

phase space process, are considered by performing alternative fits and taking the maximum value of N^{UL} as the upper limit, while the other systematic uncertainties are taken into account by dividing the factor $(1 - \delta_{\text{sys}})$, where δ_{sys} is total systematic uncertainties, described in detail later. With the detection efficiency obtained from the dedicated MC simulation for each Z_s hypothesis, the upper limit on the cross section is calculated with

$$\sigma_{Z_s}^{\text{UL}}(e^+e^- \rightarrow Z_s\pi, Z_s \rightarrow \phi\pi) = \frac{N^{\text{UL}}}{\mathcal{L}(1 + \delta)(1 - \delta_{\text{sys}})\epsilon\mathcal{B}}, \quad (1)$$

where \mathcal{L} is the integrated luminosity of the data taken at 2.125 GeV, and determined to be $(108.49 \pm 0.75) \text{ pb}^{-1}$ [21] from large-angle Bhabha scattering events; $(1 + \delta)$ is a radiative correction factor calculated to the second-order in QED [33] by assuming that the line shape follows the measured cross section of the BABAR experiment [25], determined as 0.982 and 0.986 for the $e^+e^- \rightarrow \phi\pi^+\pi^-$ and $\phi\pi^0\pi^0$ channels, respectively; ϵ is the detection efficiency; and \mathcal{B} is either $\mathcal{B}(\phi \rightarrow K^+K^-)$ for $\phi\pi^+\pi^-$ or $\mathcal{B}(\phi \rightarrow K^+K^-) \times \mathcal{B}^2(\pi^0 \rightarrow \gamma\gamma)$ for $\phi\pi^0\pi^0$ [26]. The corresponding upper limits on the differential cross sections of Z_s production as a function of the assumed mass of Z_s with different width scenario are shown in Figs. 5(a) and 5(b).

In addition, we performed the alternative amplitude analysis by assuming $J^P = 1^-$ to explore the Z_s contribution to the data. With the same approach as described above, the upper limits on the differential cross sections of Z_s production as a function of the assumed mass of Z_s with different width scenario are also estimated at 90% C.L., which are displayed in Figs. 5(c) and 5(d).

The $e^+e^- \rightarrow \phi\pi\pi$ signal yields are obtained from extended unbinned maximum likelihood fits to the $M(K^+K^-)$ distributions. In the fit, the ϕ peak is modeled as the signal MC simulated shape convoluted with a Gaussian function to account for the mass resolution difference between data and MC simulation, while the background is described by a second-order polynomial function. The fits to $M(K^+K^-)$ spectra, shown in Figs. 1(a) and 1(b), yield $(9421 \pm 138) \phi\pi^+\pi^-$ and (1649 ± 60)

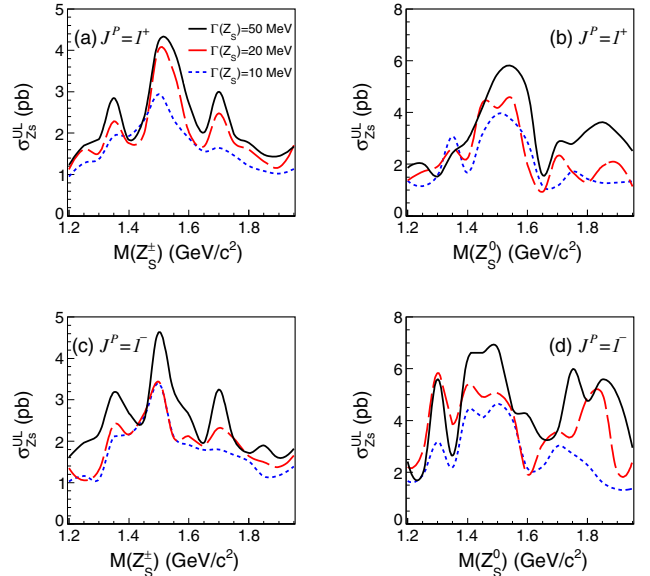


FIG. 5. The upper limits at 90% C.L. on the differential cross sections of Z_s as a function of assumed signal peak mass for the cases (a) $J^P = 1^+$ of Z_s^+ , (b) $J^P = 1^+$ of Z_s^0 , (c) $J^P = 1^-$ of Z_s^+ , and (d) $J^P = 1^-$ of Z_s^0 . The dotted, dashed and solid lines are the results of $\Gamma = 10, 20,$ and 50 MeV, respectively.

TABLE I. Systematic uncertainties (in %) for the measurements of the upper limits (uncorrelated ones) and cross sections. Assuming the uncertainties are uncorrelated, the total uncertainty is the quadratic sum of the individual values.

Source	Z_s^\pm	$\phi\pi^+\pi^-$	Z_s^0	$\phi\pi^0\pi^0$
MDC tracking	4.5	4.5	1.5	1.5
Photon detection	4	4
K PID	3	3	3	3
π PID	2	2
Kinematic fit	2.1	2.1	0.1	0.1
π^0 mass window	0.1	0.1
K^+K^- mass window	1.5	...	1.5	...
Fitting range	...	0.1	...	1.4
Signal shape	...	1.5	...	2.3
Background shape	...	1.3	...	2.0
Model uncertainty	...	0.8	...	1.3
Branching fractions	1.0	1.0	1.0	1.0
Integrated luminosity	0.7	0.7	0.7	0.7
ISR	1.0	1.0	0.7	0.7
Total	6.5	6.9	5.6	6.5

$\phi\pi^0\pi^0$ events. The detection efficiencies are $(41.2 \pm 0.1)\%$ and $(13.7 \pm 0.1)\%$, respectively, obtained from the signal MC samples generated according to the nominal amplitude analysis results. The cross sections for $e^+e^- \rightarrow \phi\pi^+\pi^-$ and $e^+e^- \rightarrow \phi\pi^0\pi^0$ are determined to be (436.2 ± 6.4) pb and (237.0 ± 8.6) pb, respectively.

Sources of systematic uncertainties and their corresponding contributions to the measurements of the cross sections are summarized in Table I. The uncertainties of the MDC tracking efficiency for each charged kaon and pion and the photon selection efficiency are studied with a control sample $e^+e^- \rightarrow K^+K^-\pi^+\pi^-$ taken at the energy of 2.125 GeV and a control sample of $e^+e^- \rightarrow \pi^+\pi^-\pi^0$ taken at the energy of 3.097 GeV, respectively, and the differences between data and MC simulation are less than 1.5% per charged track and 1.0% per photon. Similarly, the uncertainties related to the pion and kaon PID efficiencies are also studied with the sample $e^+e^- \rightarrow K^+K^-\pi^+\pi^-$, and the average differences of the PID efficiencies between data and MC simulation are determined to be 3% and 1% for each charged kaon and pion, respectively, which are taken as the systematic uncertainties.

Uncertainties associated with kinematic fits come from the inconsistency of the track helix parameters between data and MC simulation. The helix parameters for the charged tracks of MC samples are corrected to eliminate the inconsistency, as described in Ref. [34], and the agreement of χ^2 distributions between data and MC simulation is much improved. We take half of the differences on the selection efficiencies with and without the correction as the systematic uncertainties, which are 2.1% for $\phi\pi^+\pi^-$ and 0.1% for $\phi\pi^0\pi^0$ channels, respectively. The difference of the selection efficiencies associated with the π^0 mass

window requirement between data and MC simulation is estimated to be about 0.1%, which is taken as the systematic uncertainty for the mode $e^+e^- \rightarrow \phi\pi^0\pi^0$. The systematic uncertainty on the Z_s production associated with the $M(K^+K^-)$ mass window is estimated by alternative fits varying the cut by 1σ and found to be 1.5%.

In the measurement of the cross section for $e^+e^- \rightarrow \phi\pi\pi$, the nominal fit range for $M(K^+K^-)$ is $(0.99, 1.09)$ GeV/ c^2 . Alternative fits are performed by varying the fitting range. The maximum changes on the calculated cross sections are assigned as the uncertainties from the fitting range. The uncertainties associated with the background shape in the fits to $M(K^+K^-)$ are estimated with alternative fits by changing the second-order polynomial function to a third-order Chebychev polynomial function. Alternative fits to $M(K^+K^-)$ are performed by removing the smeared resolution function to estimate the uncertainties associated with the ϕ signal shape. The resultant differences are assigned as the systematic uncertainties. In the amplitude analysis, alternative fits are performed by varying the parameters of resonances according to the previous BES results [30,31] or replacing the component of $f_0(1370)$ intermediate state with a phase space process with $J^{PC} = 0^{++}$. The model with the maximum changes on the log-likelihood values are used to estimate the systematic uncertainties associated with the model.

The branching fractions of the intermediate processes $\phi \rightarrow K^+K^-$ [$(49.2 \pm 0.5)\%$] and $\pi^0 \rightarrow \gamma\gamma$ [$(98.823 \pm 0.034)\%$] are taken from the PDG [26], where the overall uncertainty, 1.0%, is taken as the systematic uncertainty. The luminosity is determined to be (108.49 ± 0.75) pb $^{-1}$ in Ref. [21] with an uncertainty of 0.7%. Uncertainties in the $Y(2125)$ resonance parameters and possible distortions of the $Y(2125)$ line shape introduce small systematic uncertainties in the radiative correction factor and the efficiency. This is estimated using the different line shapes measured by *BABAR* and *Belle*, and the difference in $(1 + \delta) \cdot \epsilon$ are taken as a systematic error, 1.0% for $e^+e^- \rightarrow \phi\pi^+\pi^-$ and 0.7% for $e^+e^- \rightarrow \phi\pi^0\pi^0$, respectively.

In summary, a search for a strangeoniumlike structure, Z_s , in the process $e^+e^- \rightarrow \phi\pi\pi$ is performed using 108 pb $^{-1}$ of data collected with the BESIII detector at 2.125 GeV. No Z_s signal is observed in the $\phi\pi$ invariant mass spectrum, and corresponding upper limits on the cross sections of Z_s production at the 90% C.L. are determined for different mass and width hypotheses, as displayed in Fig. 5. The results around 1.4 GeV/ c^2 indicate the ISPE mechanism at $K^*\bar{K}$ threshold is not as significant as predicted in Ref. [22]. Further study with larger statistics is essential to examine the existence of the Z_s structure and test the ISPE mechanism.

In addition, the cross sections for $e^+e^- \rightarrow \phi\pi^+\pi^-$ and $e^+e^- \rightarrow \phi\pi^0\pi^0$ are determined to be $(436.2 \pm 6.4 \pm 30.1)$ pb and $(237.0 \pm 8.6 \pm 15.4)$ pb, respectively. The measured cross sections are consistent with previous

measurements from the *BABAR* ($510 \pm 50 \pm 21$ pb at 2.1125 GeV for $e^+e^- \rightarrow \phi\pi^+\pi^-$ and $195 \pm 50 \pm 14$ pb at 2.100 GeV for $e^+e^- \rightarrow \phi\pi^0\pi^0$) [25] and Belle experiments ($480 \pm 60 \pm 42$ pb at 2.1125 GeV for $e^+e^- \rightarrow \phi\pi^+\pi^-$) [35] within uncertainties. For both measurements, the statistical uncertainties are reduced significantly.

The BESIII Collaboration thanks the staff of BEPCII and the IHEP computing center for their strong support. This work is supported in part by National Key Basic Research Program of China under Contract No. 2015CB856700; National Natural Science Foundation of China (NSFC) under Contracts No. 11235011, No. 11335008, No. 11425524, No. 11625523, No. 11635010, No. 11675184, No. 11505034, No. 11575077, and No. 11735014; the Chinese Academy of Sciences (CAS) Large-Scale Scientific Facility Program; Youth Science Foundation of China under Contract No. Y5118T005C; the CAS Center for Excellence in Particle Physics (CCEPP); Joint Large-Scale Scientific Facility Funds of the NSFC and CAS under Contracts

No. U1332201, No. U1532257, and No. U1532258; CAS under Contracts No. KJCX2-YW-N29, No. KJCX2-YW-N45, and No. QYZDJ-SSW-SLH003; 100 Talents Program of CAS; National 1000 Talents Program of China; INPAC and Shanghai Key Laboratory for Particle Physics and Cosmology; German Research Foundation DFG under Contracts Nos. Collaborative Research Center CRC 1044, FOR 2359; Istituto Nazionale di Fisica Nucleare, Italy; Koninklijke Nederlandse Akademie van Wetenschappen (KNAW) under Contract No. 530-4CDP03; Ministry of Development of Turkey under Contract No. DPT2006K-120470; National Science and Technology fund; The Swedish Research Council; U. S. Department of Energy under Contracts No. DE-FG02-05ER41374, No. DE-SC-0010118, No. DE-SC-0010504, and No. DE-SC-0012069; University of Groningen (RuG) and the Helmholtzzentrum fuer Schwerionenforschung GmbH (GSI), Darmstadt; and the WCU Program of National Research Foundation of Korea under Contract No. R32-2008-000-10155-0.

-
- [1] M. Ablikim *et al.* (BESIII Collaboration), *Phys. Rev. Lett.* **110**, 252001 (2013).
- [2] Z. Q. Liu *et al.* (Belle Collaboration), *Phys. Rev. Lett.* **110**, 252002 (2013).
- [3] M. Ablikim *et al.* (BESIII Collaboration), *Phys. Rev. Lett.* **111**, 242001 (2013).
- [4] M. Ablikim *et al.* (BESIII Collaboration), *Phys. Rev. Lett.* **112**, 132001 (2014).
- [5] M. Ablikim *et al.* (BESIII Collaboration), *Phys. Rev. Lett.* **112**, 022001 (2014).
- [6] K. Chilikin *et al.* (Belle Collaboration), *Phys. Rev. D* **90**, 112009 (2014).
- [7] A. Roel *et al.* (LHCb Collaboration), *Phys. Rev. Lett.* **112**, 222002 (2014).
- [8] L. Maiani, V. Riquer, R. Faccini, F. Piccinini, A. Pilloni, and A. D. Polosa, *Phys. Rev. D* **87**, 111102 (2013).
- [9] G. T. Bodwin *et al.*, arXiv:1307.7425.
- [10] M. B. Voloshin, *Phys. Rev. D* **87**, 091501(R) (2013).
- [11] N. Brambilla *et al.*, *Eur. Phys. J. C* **74**, 2981 (2014).
- [12] X. Liu, *Chin. Sci. Bull.* **59**, 3815 (2014).
- [13] F.-K. Guo, C. Hidalgo-Duque, J. Nieves, and M. Pavon Valderrama, *Phys. Rev. D* **88**, 054007 (2013).
- [14] A. Esposito, A. L. Guerrieri, F. Piccinini, A. Pilloni, and A. D. Polosa, *Int. J. Mod. Phys. A* **30**, 1530002 (2015).
- [15] M. Ablikim *et al.* (BESIII Collaboration), *Phys. Rev. Lett.* **113**, 212002 (2014).
- [16] M. Ablikim *et al.* (BESIII Collaboration), *Phys. Rev. Lett.* **115**, 112003 (2015).
- [17] M. Ablikim *et al.* (BESIII Collaboration), *Phys. Rev. Lett.* **115**, 182002 (2015).
- [18] M. Ablikim *et al.* (BESIII Collaboration), *Phys. Rev. Lett.* **115**, 222002 (2015).
- [19] G. J. Ding and M. L. Yan, *Phys. Lett. B* **650**, 390 (2007).
- [20] S. Okubo, *Phys. Lett.* **5**, 165 (1963); G. Zweig, CERN Report No. 8419/TH412, 1964; J. Iizuka, *Prog. Theor. Phys. Suppl.* **37**, 21 (1966).
- [21] M. Ablikim *et al.* (BESIII Collaboration), *Chin. Phys. C* **41**, 113001 (2017).
- [22] D. Y. Chen, X. Liu, and T. Matsuki, *Eur. Phys. J. C* **72**, 2008 (2012).
- [23] M. Ablikim *et al.* (BESIII Collaboration), *Nucl. Instrum. Methods Phys. Res., Sect. A* **614**, 345 (2010).
- [24] S. Agostinelli *et al.*, *Nucl. Instrum. Methods Phys. Res., Sect. A* **506**, 250 (2003).
- [25] J. P. Lees *et al.* (*BABAR* Collaboration), *Phys. Rev. D* **86**, 012008 (2012).
- [26] C. Patrignani *et al.* (Particle Data Group), *Chin. Phys. C* **40**, 100001 (2016).
- [27] B. S. Zou and D. V. Bugg, *Eur. Phys. J. A* **16**, 537 (2003).
- [28] B. S. Zou and D. V. Bugg, *Phys. Rev. D* **48**, R3948 (1993).
- [29] S. M. Flatté, *Phys. Lett.* **63B**, 224 (1976).
- [30] M. Ablikim *et al.* (BES Collaboration), *Phys. Lett. B* **607**, 243 (2005).
- [31] M. Ablikim *et al.* (BES Collaboration), *Phys. Lett. B* **598**, 149 (2004).
- [32] M. Ablikim *et al.* (BESIII Collaboration), *Phys. Rev. D* **95**, 032002 (2017).
- [33] E. A. Kuraev and V. S. Fadin, *Yad. Fiz.* **41**, 733 (1985) [*Sov. J. Nucl. Phys.* **41**, 466 (1985)]; R. G. Ping, *Chin. Phys. C* **38**, 083001 (2014).
- [34] M. Ablikim *et al.* (BESIII Collaboration), *Phys. Rev. D* **87**, 012002 (2013).
- [35] C. P. Shen *et al.* (Belle Collaboration), *Phys. Rev. D* **80**, 031101 (2009).